Brönsted and Lewis Acidity of the BF_3/γ-Al_2O_3 Alkylation Catalyst as Revealed by Solid-State NMR Spectroscopy and DFT Quantum Chemical Calculations

Jun Yang,[†] Anmin Zheng,[†] Mingjin Zhang,[†] Qing Luo,[†] Yong Yue,[†] Chaohui Ye,[†] Xin Lu,[‡] and Feng Deng*,[†]

State Key Laboratory of Magnetic Resonance and Atomic and Molecular Physics, Wuhan Institute of Physics and Mathematics, The Chinese Academy of Sciences, Wuhan 430071, People's Republic of China, and State Key Laboratory of Physical Chemistry of Solid Surface, Xiamen University, Xiamen 361005, People's Republic of China

Received: March 11, 2005; In Final Form: May 10, 2005

Multinuclear solid-state NMR techniques and DFT quantum chemical calculations were employed to investigate the detailed structure of acid sites on the BF_3/γ-Al_2O_3 alkylation catalyst. The NMR experiment results indicate that gaseous BF_3 is able to react with the hydroxyl groups present on the surface of γ-Al_2O_3, leading to the formation of new Brönsted and Lewis acid sites. The $^1H/^{11}B$ and $^1H/^{27}Al$ TRAPDOR (TRAnsfer of Population in DOuble Resonance) experiments suggest that the 3.7 ppm signal in ^1H NMR spectra of the BF_3/γ-Al_2O_3 catalyst is due to a bridging B−OH−Al group that acts as a Brönsted acid site of the catalyst. On the other hand, a Lewis acid site on the surface of the catalysts, as revealed by ^{31}P MAS and $^{31}P/^{27}Al$ TRAPDOR NMR of adsorbed trimethylphosphine, is associated with three-coordinate $-OBF_2$ species. ^{13}C NMR of adsorbed 2-^{13}C-acetone indicates that the Brönsted acid strength of the catalyst is slightly stronger than that of zeolite HZSM-5 but still weaker than that of 100% H_2SO_4, which is in good agreement with theoretical prediction. In addition, DFT calculations also reveal the detailed structure of various acid sites formed on the BF_3/γ-Al_2O_3 catalyst and the interaction of probe molecules with these sites.

Introduction

Alkylation of isobutane with butene produces the important component of high-octane and clean-burning gasoline. The product, alkylate, has a high octane number and a low Reid vapor pressure. Industrial alkylation processes are using sulfuric acid and hydrofluoric acid as acid catalysts. The liquid acid alkylation catalysts are highly toxic, corrosive, and dangerous to life or health during their use and transportation. The problems have raised interest in developing nontoxic, noncorrosive, easy to handle, and environmentally friendly solid acid alkylation catalysts.[1−3]

Many different types of solid acid have been studied both in industry and in academic institutions as isobutene alkylation catalysts. These catalysts include zeolite,[4] heteropolyacids,[5] sulfated oxide,[6] catalyst containing halogen[7] (such as BF_3/γ-Al_2O_3), and immobilized liquid acid[7] (such as CF_3SO_3H). Among them, zeolite and sulfated zirconia have been extensively studied. It has been accepted that most zeolites are not suitable for alkylation due to the broad distribution of their acid strengths. Liquid acid alkylation catalysts, such as sulfuric acid, usually have a narrow and strong acidity, whereas most of the large microporous zeolites (such as faujasite and β-zeolite) do not hold this acidic property. Sulfated zirconia shows a high initial activity, but the catalyst is quickly deactivated with time on stream.

BF_3/γ-Al_2O_3 is one of the most promising alkylation catalysts for HF replacement. In 1994, Catalytica Advanced Technologies set up a demonstration alkylation unit in Finland using BF_3/γ-Al_2O_3 as the alkylation catalyst.[7] In contrast to the extensive study of the zeolites and sulfated zirconia, investigation of BF_3/γ-Al_2O_3 is rarely carried out. As a potential alkylation catalyst, the structure and nature of acid sites on the BF_3/γ-Al_2O_3 solid acid catalyst are still unclear, though there are many patents concerned with the preparation and catalytic performance of the catalyst. Some of the patent literature seems to assume that the BF_3 is physisorbed onto the surface of γ-Al_2O_3.[8] However, strong Brönsted acid sites may be formed by reaction between BF_3 and the hydroxyl groups present on the surface of γ-Al_2O_3. Recently, Drago et al.[9] observed Brönsted acid sites on a catalyst formed by the deposition of aluminum chloride onto silica, and they proposed a bridging structure analogous to the bridging hydroxyl of zeolites. In a previous investigation,[10] Hammett indicator tests indicated that the BF_3/γ-Al_2O_3 was a superacid with an acid strength higher than 100% sulfuric acid. However, according to the recent spectroscopic results,[11] the application of the Hammett formalism related to the strength of solid acids is not strictly valid. For example, zeolites were previously classified as superacids, since their Hammett acidity was stronger than 100% sulfuric acid. However, spectroscopic studies of reaction intermediates and probe molecules adsorbed on zeolites have demonstrated that the acid strengths of zeolites are considerably weaker than those of superacids.[11]

Solid-state NMR has proven to be a powerful technique for investigating the acid properties of various solid acid catalysts.[12−15] In addition, theoretical calculations have been successfully employed to predict the structure and acidity of the solid acids.[11] Haw et al.[13−16] have calculated the proton affinity (PA) and ^{13}C chemical shift of 2-^{13}C-acetone absorbed on various solid acids, such as zeolite HZSM-5, $AlCl_3/SiO_2$, SO_3/SiO_2, and

* To whom correspondence should be addressed. E-mail: dengf@wipm.ac.cn. Fax: +86-27-87199291.
[†] Wuhan Institute of Physics and Mathematics.
[‡] Xiamen University.

10.1021/jp051268l CCC: $30.25
Published on Web 06/18/2005

sulfated zirconia catalysts, and predicted the acid strength of the solid acids by the magnitude of the PA and ^{13}C chemical shift. It is well-known that the smaller the PA and the larger the ^{13}C chemical shift of 2-^{13}C-acetone means the stronger acid strength of Brönsted acidity. In this study, we employed ^{1}H, ^{19}F, ^{11}B, and ^{27}Al MAS NMR and double resonance techniques to study the detailed structure of acid sites formed after the adsorption of BF_3 onto γ-Al_2O_3. ^{13}C and ^{31}P NMR techniques of adsorbed probe molecules, such as 2-^{13}C-acetone and trimethylphosphine (TMP), were used to determine the type and strength of acid sites on the BF_3/γ-Al_2O_3 catalyst. In addition, density functional theory (DFT) calculations were used to clarify the detailed structure of Brönsted and Lewis acid sites proposed on the basis of the NMR experimental results and to predict their acid strengths.

Experimental Section

Sample Preparation. BF_3/γ-Al_2O_3 was prepared by the adsorption of gaseous BF_3 onto the surface of activated γ-Al_2O_3 in an autoclave at 573 K for 4 h and then calcination in flow air at 673 K for 2 h.[17] Prior to ^{1}H MAS NMR experiments and the adsorption of probe molecules, the samples were dehydrated at 673 K under pressure below 10^{-3} Pa for 5 h on a vacuum line. TMP (50 Torr) was introduced onto the activated catalyst and equilibrated for 1 h and then degassed for 1 h at room temperature. A known amount of 2-^{13}C-acetone was introduced and frozen on the activated catalyst with liquid N_2. The sealed samples were transferred into a ZrO_2 rotor (sealed by a Kel-F cap) under a dry nitrogen atmosphere in a glovebox.

NMR Spectroscopy. All of the NMR experiments were carried out at 9.4 T on a Varian Infinityplus-400 spectrometer at room temperature. ^{1}H MAS NMR spectra were recorded with a spin−echo pulse sequence. Single pulse ^{31}P MAS NMR experiments with ^{1}H decoupling were performed with an 8 s recycle delay. $^{1}H-^{13}C$ CP/MAS spectra were recorded with a 2 ms contact time and a 2 s recycle delay. The TRAPDOR experiments were performed according to the method proposed by Grey et al.[18] $^{1}H/^{27}Al$ and $^{1}H/^{11}B$ TRAPDOR experiments were carried out with a spinning speed of 6 kHz, irradiation time of 500 μs (three rotor periods), and radio frequency (rf) field strengths of 62.5 and 54 kHz for ^{27}Al and ^{11}B, respectively. The $^{31}P/^{27}Al$ TRAPDOR experiments were measured with a spinning rate of 4 kHz, an ^{27}Al irradiation time of 500 μs (two rotor periods), and a rf field strength of 62.5 kHz. The ^{27}Al and ^{11}B 3Q-MAS spectra were recorded with the pulse sequence proposed by Amoureux et al.[19] The quadrupolar coupling constant (Qcc) and asymmetry factor (η) of the ^{11}B signal were extracted from the slice of 3Q-MAS spectra by fitting the corresponding second-order quadrupolar line shape with the dmfit program.[20] The $^{11}B/^{27}Al$ REDOR experiment was carried out using a standard REDOR pulse sequence,[21] with and without applying rotor-synchronized π pulses to the ^{27}Al channel within 48 rotor cycles. In the REDOR experiment including half-integral quadrupolar nuclei, selective pulses ($\pi/2$ or π) were used to excite the central $1/2 \leftrightarrow -1/2$ transition of ^{11}B (or ^{27}Al). The following parameters were used: spinning speed, 10 000 ± 2 Hz; selective π pulse length, 10.8 μs for ^{11}B and 13.6 μs for ^{27}Al, respectively. The ^{1}H, ^{19}F, ^{31}P, ^{13}C, ^{27}Al, and ^{11}B NMR chemical shifts were externally referenced to TMS, D-trifluoroacetic acid, 85% H_3PO_4 solution, hexamethylbenzene, 0.1 M $Al(NO_3)_3$ solution, and H_3BO_3 solution, respectively.

Theoretical Calculation Method

Two possible models (I and II) including a six-membered ring were proposed for the Brönsted acid sites formed on the BF_3/γ-Al_2O_3 catalyst. We used a cluster model containing eight

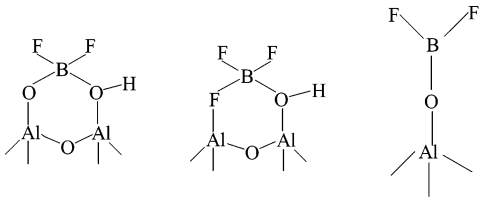

model I model II model III

aluminum atoms for the calculations, and the structure parameters for building the cluster were derived from part of the crystal structure of γ-Al_2O_3,[22] which includes both octahedral (Al_O) and tetrahedral aluminum (Al_T) sites. During the structure optimization, only the atoms located in the six-membered rings were allowed to relax, while all the rest of the atoms were keep fixed at their crystallographic locations. This partial optimization method is essential to avoid an unrealistic collapse of the γ-Al_2O_3 structure and has been widely used in the calculations of zeolite.[14,16] Each peripheral Al atom is saturated with hydrogen atoms in the calculations, and the terminal Al atoms are located at an Al−H distance of 1.55 Å from the corresponding oxygen, orienting along the bond direction to the next oxygen atom in the X-ray diffraction (XRD) structure. No atom in the adsorbed acetone molecule was constrained in the optimization of adsorption complex model. Our calculations include the structure optimization, single point energy, zero point energy, and thermal energy correction, as well as the ^{13}C NMR chemical shift of adsorbed acetone, and the hybrid density functional B3LYP method was employed with standard DZVP2 basis sets. The NMR parameters were calculated by the GIAO method. The calculated ^{13}C NMR isotropic chemical shift of the carbonyl carbon of acetone absorption complexes was referenced to that of the NMR experimental value of the gas state acetone (208 ppm). The possible structure of the Lewis acid site on BF_3/γ-Al_2O_3 was proposed on the basis of our NMR experimental results as well (model III). The complex structures of TMP with Lewis acid sites of both the BF_3/γ-Al_2O_3 and the parent γ-Al_2O_3 catalysts were optimized, and their ^{31}P isotropic chemical shifts were calculated by the GIAO method. The ^{31}P isotropic chemical shift was referenced to the NMR experimental value of liquid TMP (−62 ppm).[23] All of the calculations in this study were performed using the Gaussian03 program package[24] on a PC cluster.

Results and Discussion

^{1}H MAS, $^{1}H/^{27}Al$, and $^{1}H/^{11}B$ TRAPDOR NMR. ^{1}H NMR is a direct technique for characterizing Brönsted acid sites on solid acids. The ^{1}H MAS NMR spectrum of parent γ-Al_2O_3 is shown in Figure 1a. Although five different hydroxyl groups were identified in amorphous γ-alumina by the IR technique,[25a] only three types of hydroxyl groups could be resolved by ^{1}H MAS NMR:[25b] a terminal OH group attached to a single tetrahedral or octahedral Al ($OHAl_O$ or $OHAl_T$), a bridging OH coordinated to two octahedral Al ($OH2Al_O$) or to one tetrahedral Al and one octahedral Al ($OHAl_OAl_T$), and a bridging OH attached to three octahedral Al ($OH3Al_O$), giving rise to ^{1}H signals at approximately 0, 2.5, and 4.3 ppm, respectively.[25b] A similar assignment can be made for the 0.3 and 2.2 ppm signals and the shoulder peak at the low-field region of the 2.2 ppm signal in our ^{1}H NMR spectra. Adsorption of BF_3 onto the surface of γ-Al_2O_3 results in substantial changes in the

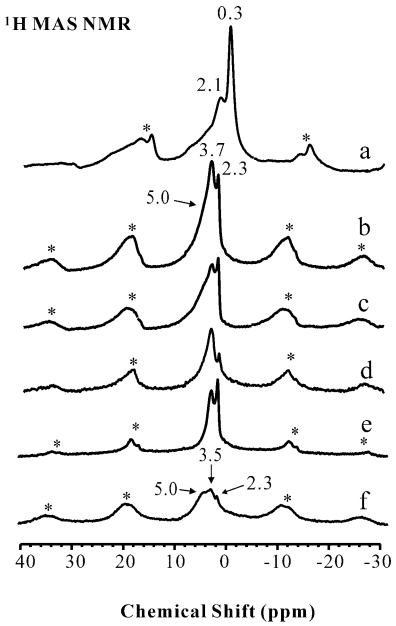

Figure 1. ^{1}H spin−echo spectra of (a) γ-Al_2O_3 (without Al irradiation), (b) BF_3/γ-Al_2O_3 (without Al or B irradiation), (c) BF_3/γ-Al_2O_3 (with 500 μs B irradiation, rf field strength = 54 kHz), (d) difference spectrum of parts b and c, (e) BF_3/γ-Al_2O_3 (with 500 μs Al irradiation, rf field strength = 62.5 kHz), (f) difference spectrum of parts b−e. A MAS spinning speed of 6 kHz was used. Asterisks denote spinning sidebands.

corresponding ^{1}H spectrum (Figure 1b). The most apparent change is that the 0.3 ppm signal disappears completely, indicating that BF_3 reacts preferentially with the most basic OH groups (0.3 ppm). Another change is that a new signal at ~3.7 ppm with a shoulder peak at ~5.0 ppm appears and dominates the spectrum.

To reveal the nature of these signals, we carried out ^{1}H/^{11}B and ^{1}H/^{27}Al TRAPDOR experiments. The experiments are analogous to dipolar dephasing experiments. Under ^{11}B (or ^{27}Al) irradiation, the signals of protons that are strongly coupled with boron (or aluminum) atoms will be significantly suppressed, whereas those that are not coupled with boron (or aluminum) atoms will remain unaffected. Hence, it is a measure of the heteronuclear dipolar interaction between a half-integer quadrupole nucleus and an $I = 1/2$ nucleus. Under on-resonance ^{11}B irradiation, the two signals at 3.7 and 2.3 ppm are partially reduced, while the shoulder peak remains almost unchanged (Figure 1c and d), suggesting that only the former two signals show TRAPDOR effects and the corresponding hydroxyl groups are all in close proximity to the boron atom. Similarly, the ^{1}H/^{27}Al TRAPDOR experiment (Figure 1e and f) indicates that the hydroxyl groups corresponding to the 3.7 and 2.3 ppm signals are also associated with Al atoms. It is noteworthy that the shoulder peak at 5.0 ppm shows a detectable TRAPDOR effect as well (Figure 1f), implying that the corresponding hydroxyl groups are associated with Al rather than B atoms. According to the chemical shifts of these signals and the TRAPDOR experimental results, we ascribe the 3.7 ppm signal to bridging Al−OH−B hydroxyl groups, analogous to the bridging Si−OH−Al groups in zeolites, and the 2.3 ppm signal to an AlOH group associated with BF_3 or $-OBF_2$ species through H···F hydrogen bonding. The $-OBF_2$ species is formed by the reaction of BF_3 with the AlOH group of γ-Al_2O_3 through the elimination of one HF molecule. As will be seen in the following, our ^{11}B/^{27}Al REDOR experiment demonstrates that adsorbed three-coordinate BF_3 is absent on the BF_3/γ-Al_2O_3 catalyst. Therefore, we assign the 2.3 ppm signal to the $-OBF_2$ species. The 5.0 ppm signal was assigned to water adsorbed on the surface of γ-Al_2O_3 in a previous paper.[26] Since this signal possesses relatively strong spinning sidebands and only shows a strong ^{1}H/^{27}Al TRAPDOR effect, the corresponding adsorbed water molecules might be less mobile and tightly bound to Al atoms. Indeed, this signal can also be resolved in the ^{1}H NMR spectrum (not shown) of parent γ-Al_2O_3 acquired by using a ^{1}H spin−echo pulse sequence with an echo time larger than 2 ms. Therefore, we are unable to rule out the possibility that this signal arises from the Al−OH group that is originally present on the surface of parent γ-Al_2O_3. After the adsorption of BF_3 onto γ-Al_2O_3, the 0.3 ppm signal is selectively removed and the 5.0 ppm signal becomes evident.

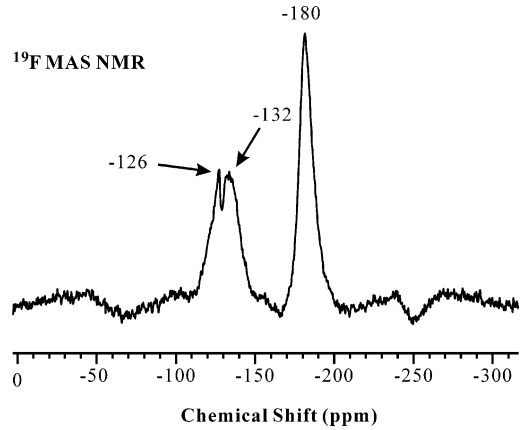

Figure 2. ^{19}F MAS NMR spectrum of the BF_3/γ-Al_2O_3 catalyst. A MAS spinning speed of 25 kHz was used.

SCHEME 1

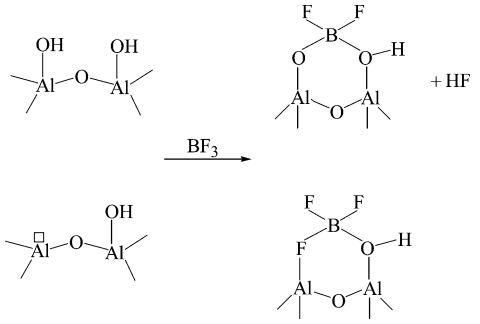

^{19}F MAS NMR. The ^{19}F MAS NMR spectrum of the BF_3/γ-Al_2O_3 sample is shown in Figure 2. Since a fast spinning speed (25 kHz) was used, overlapping of observed signals with their spinning sidebands could be avoided. Three signals are present in the ^{19}F MAS NMR spectrum. According to the literature,[27] the signal at −180 ppm can be assigned to F atoms directly coupled to Al atoms, which is likely formed by the coordination of a F atom of BF_3 with an unsaturated defect Al site present on the surface of γ-Al_2O_3 (see Scheme 1). The presence of an Al−F bond is also confirmed by ^{27}Al MAS NMR spectroscopy (see the following). The two signals at −130 and −126 ppm can be attributed to an $-OBF_2$ species that is formed by the reaction of BF_3 with AlOH groups of γ-Al_2O_3 (Schemes 1 and 2).

^{11}B, ^{27}Al MAS, and MQ-MAS NMR. ^{11}B and ^{27}Al MAS NMR can provide direct information about the coordination state of boron and aluminum species in the BF_3/γ-Al_2O_3 catalyst. In ^{11}B MAS NMR spectra, the four-coordinate boron signal usually gives rise to an isotropic chemical shift at ~0 ppm and a relatively narrow Gaussian line shape, while the three-coordinate boron signal is centered at ~15 ppm with a typical second-

SCHEME 2

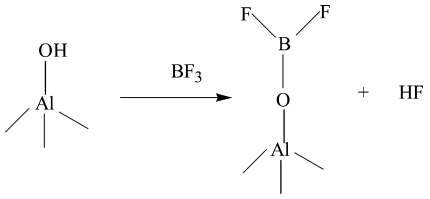

order quadrupole line shape. The second-order quadrupole interaction cannot be completely averaged by magic angle spinning. With the introduction of the multiple-quantum magic angle spinning (MQMAS) experiment by Frydman and Harwood,[28] high-resolution isotropic spectra of half-integer quadrupolar nuclei can be obtained. In a MQMAS experiment, the second-order anisotropic broadening is refocused and an isotropic dimension, free of anisotropic quadrupolar interactions, can be obtained. Figure 3 shows the ^{11}B MAS and MQ-MAS NMR spectra of the BF_3/γ-Al_2O_3 catalyst. Obviously, two separate signals (A and B) can be well resolved in the MQ-MAS spectrum. By spectral simulation with the help of the MQMAS data, we found that the MAS spectrum consisted of a typical second-order quadrupolar pattern with a δ_{iso} value of $\sim$15.3 ppm, a quadrupolar coupling constant (Qcc) of $\sim$2.8 MHz, and an η_Q value of 0.3, arising from three-coordinate boron, and a sharp line δ_{iso} at $\sim$0 ppm, due to four-coordinate boron. It can be expected that the formation of four-coordinate boron is most likely due to the reaction of BF_3 with the hydroxyl groups on the surface of γ-Al_2O_3.

Two signals at 68 and 8 ppm are present in the ^{27}Al MAS NMR spectrum (Figure 4a) of parent γ-Al_2O_3, which can be assigned to four- and six-coordiante Al, respectively. After the adsorption of BF_3 onto the surface of γ-Al_2O_3, a new shoulder peak at ~ -16 ppm appears (Figure 4b). According to the literature,[27] the signal at this chemical shift range is due to an octahedral aluminum oxyfluoride group, such as $AlO_{6-x}F_x$. The assignment of this signal is quite consistent with the corresponding ^{19}F NMR experimental result. Probably due to the relatively small quadrupole interaction of the ^{27}Al signals, the shoulder peak is not resolved in the corresponding ^{27}Al MQ-MAS spectrum (Figure 4c).

^{11}B/^{27}Al REDOR NMR. The rotational echo double resonance (REDOR) technique originally proposed by Gullion and Schaefer[21] is a double resonance NMR technique for establishing spatial correlation between neighboring nuclei through recoupling the heteronuclear dipolar coupling. Figure 5 shows the ^{11}B/^{27}Al REDOR NMR spectrum of the BF_3/γ-Al_2O_3 catalyst. After the application of an irradiation with 48 rotor-synchronized π pulses on the Al channel, the intensities of the two boron signals are considerably reduced (see the difference spectrum in Figure 5c), indicating that both of them are in close proximity to Al in the BF_3/γ-Al_2O_3 catalyst. Our ^{11}B/^{27}Al REDOR NMR experiment results suggest that the reaction between BF_3 and hydroxyl on the surface of γ-Al_2O_3 occurs and a B$-$O$-$Al linkage is likely formed on the BF_3/γ-Al_2O_3 catalyst.

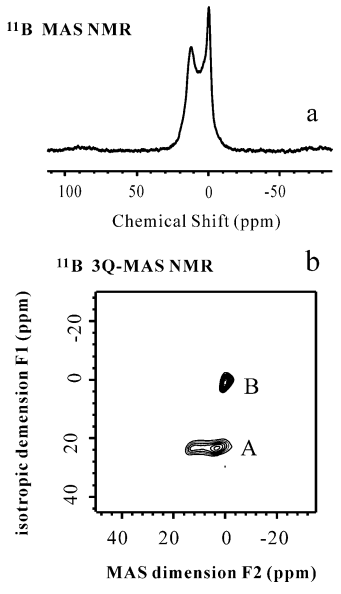

Figure 3. ^{11}B MAS (a) and 3Q-MAS (b) NMR spectra of BF_3/γ-Al_2O_3.

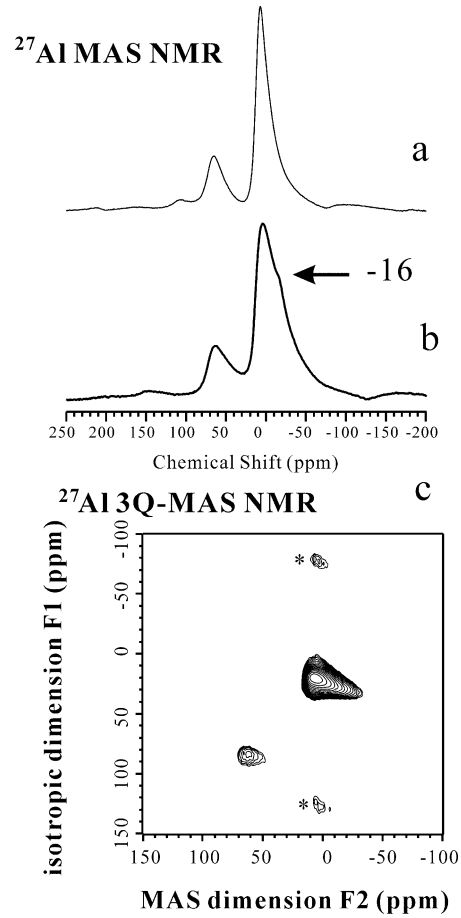

Figure 4. ^{27}Al MAS NMR spectra of (a) γ-Al_2O_3 and (b) BF_3/γ-Al_2O_3 and (c) 3Q-MAS NMR spectrum of BF_3/γ-Al_2O_3. Asterisks denote spinning sidebands.

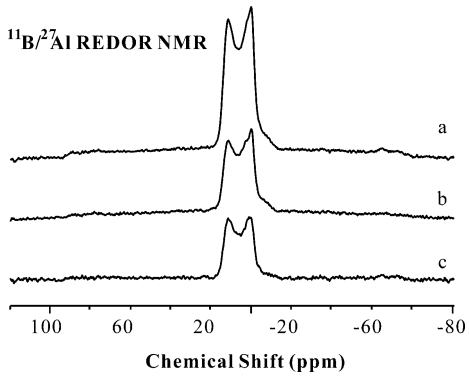

Figure 5. ^{11}B/^{27}Al REDOR NMR spectra of BF_3/γ-Al_2O_3 (a) without and (b) with the application of rotor-synchronized π pulses to the ^{27}Al channel within 48 rotor cycles, (c) difference spectrum of parts a and b. A MAS spinning speed of 10 000 $\pm$ 2 Hz was used, and the π pulse lengths were 10.8 and 13.6 μs for ^{11}B and ^{27}Al, respectively.

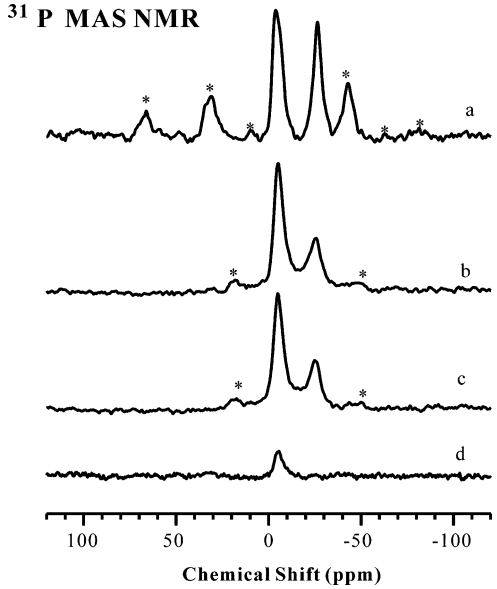

Figure 6. ^{31}P spin−echo MAS NMR spectra of TMP adsorbed on BF_3/γ-Al_2O_3 (a) without ^{1}H decoupling, (b) with ^{1}H decopupling, (c) with 500 μs ^{27}Al irradiation, rf field strength = 62.5 kHz, and (d) difference spectrum of parts b and c. A MAS spinning speed of 4 kHz was used. Asterisks denote spinning sidebands.

^{31}P and ^{31}P/^{27}Al TRAPDOR NMR of TMP Adsorbed on BF_3/γ-Al_2O_3. TMP is a widely used probe molecule for distinguishing Brönsted and Lewis acid sites on the surface of solid acid catalysts.[29] It is well accepted that the formation of $TMPH^+$ ion due to the interaction of TMP with Brönsted acid sites will give rise to a ^{31}P resonance at about −2 to −4 ppm, while TMP molecules bound to Lewis acid sites of zeolite will result in ^{31}P resonance at the shift range from −32 to −58 ppm, and physisorbed TMP molecules will give rise to a ^{31}P NMR signal at about −68 ppm. In the ^{31}P MAS spectrum of TMP adsorbed on γ-Al_2O_3, only one peak at −51 ppm due to TMP bound to a Lewis acid site was observed.[30] After the introduction of BF_3 onto the surface of γ-Al_2O_3 (Figure 6a), a strong signal at −4 ppm with intense spinning sidebands can be observed in the ^{31}P MAS NMR spectra (without ^{1}H decoupling). With ^{1}H decoupling, the spinning sidebands are considerably suppressed (Figure 6b), indicating that a strong dipolar interaction is present between the phosphorus atom of TMP and the acidic proton of the BF_3/γ-Al_2O_3 catalyst. Therefore, we suspect that protonated $TMPH^+$ ion is formed by interaction between TMP and newly generated Brönsted acid sites on the surface of BF_3/γ-Al_2O_3, such as bridging hydroxyl Al−OH−B groups. Furthermore, the −51 ppm signal in the ^{31}P NMR spectrum of parent γ-Al_2O_3 disappears completely, while a new signal at −26 ppm can be observed. Previous studies[31] demonstrated that ^{31}P signals of TMP bound to the Al-containing Lewis acid sites had a chemical shift range of −32 to −58 ppm and showed strong ^{27}Al/^{31}P TRAPDOR effects. However, in our ^{27}Al/^{31}P TRAPDOR experiments performed on the BF_3/γ-Al_2O_3 catalyst, a negligible ^{27}Al/^{31}P TRAPDOR effect is observed for the −26 ppm signal (Figure 6c and d), implying that Lewis acid sites on the surface of BF_3/γ-Al_2O_3 are not associated with Al atoms. In contrast, the −4 ppm signal shows a detectable TRAPDOR effect. The weak TRAPDOR effect is likely due to the relatively long distance between the P atom of TMP and the Al atom on the surface of BF_3/γ-Al_2O_3. Although the ^{11}B/^{31}P TRAPDOR experiment is not feasible on our spectrometer, in combination with the above ^{11}B NMR and the following DFT calculated results, we deduce that the −26 ppm signal results from TMP adsorbed on boron-containing Lewis acid sites, such as a three-coordinate boron species ($-OBF_2$) that is formed by the reaction of BF_3 with one AlOH group of γ-Al_2O_3 and subsequent removal of one HF molecule (see Scheme 2).

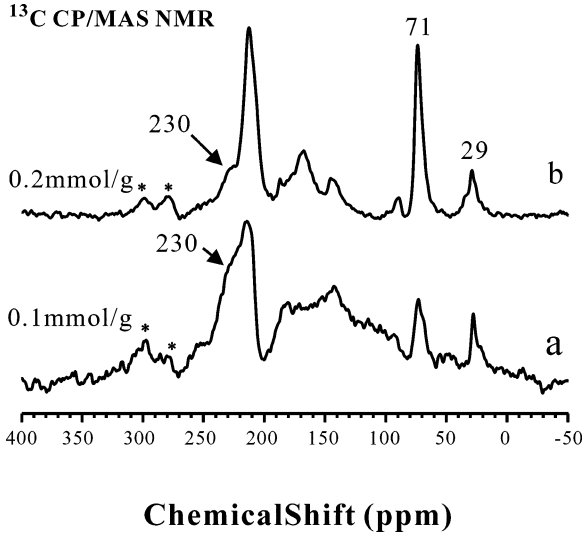

Figure 7. ^{13}C CP/MAS NMR spectra of 2-^{13}C-acetone adsorbed on BF_3/γ-Al_2O_3. The broad peaks between 120 and 180 ppm in the ^{13}C spectra are due to the background of spinning module. Asterisks denote spinning sidebands.

^{13}C NMR of Acetone Adsorbed on BF_3/γ-Al_2O_3. As demonstrated by earlier studies,[10,32] the ^{13}C isotropic chemical shift of the carbonyl carbon of 2-^{13}C-acetone can be used as a mark to evaluate the acid strength of solid acids. The stronger the Brönsted acidity, the stronger the interaction between the carbonyl carbon and the acidic proton, and consequently the more the downfield of the ^{13}C isotropic chemical shift. Therefore, 2-^{13}C-acetone is a useful NMR probe molecule for determining the relative acid strength of solid acids. After the adsorption of 0.1 or 0.2 mmol/g of acetone onto the surface of the BF_3/γ-Al_2O_3 catalyst (Figure 7a and b), besides signals at 214, 71, and 29 ppm (arising from the products of bimolecular and trimolecular reactions of acetone[32b]), we can observe a signal at 230 ppm in the CP/MAS ^{13}C NMR spectra that is due to unreacted acetone adsorbed on the acid sites. Because the signal of acetone adsorbed on the Lewis acid sites is absent in the ^{13}C NMR spectra recorded with the application of cross-polarization (CP/MAS),[12c] the signal might be due to the acetone adsorbed on Brönsted acid sites. The large chemical shift indicates that the acid strength of the BF_3/γ-Al_2O_3 catalyst is slightly stronger than the bridging OH group of zeolite HZSM-5, where adsorbed 2-^{13}C-acetone gives rise to a ^{13}C resonance at 223 ppm, but still weaker than that of 100% H_2SO_4, in which the isotropic ^{13}C shift of 2-^{13}C-acetone is ∼245 ppm.

DFT Calculations. We use the quantum chemical calculation method to obtain detailed information on the structure and nature of Brönsted and Lewis acid sites formed on the BF_3/γ-Al_2O_3 catalyst. Two models (I and II) of Brönsted acid sites and one model (III) of Lewis acid sites were considered on the basis of our NMR experimental results. Both of the Brönsted acid sites consist of a six-membered ring structure with a bridging Al−OH−B hydroxyl group.

In the optimized structure of Brönsted acid model I (Figure 8), the B−O (H) bond length is 1.674 Å and the other B−O bond length is 1.405 Å, the distance between the acidic proton and the O atom is 0.966 Å, and the bond angle of Al−OH−B is 123.1°. The proton affinity of model I is theoretically determined as the enthalpy difference between the corresponding deprotonated and protonated models. The calculated PA is 318

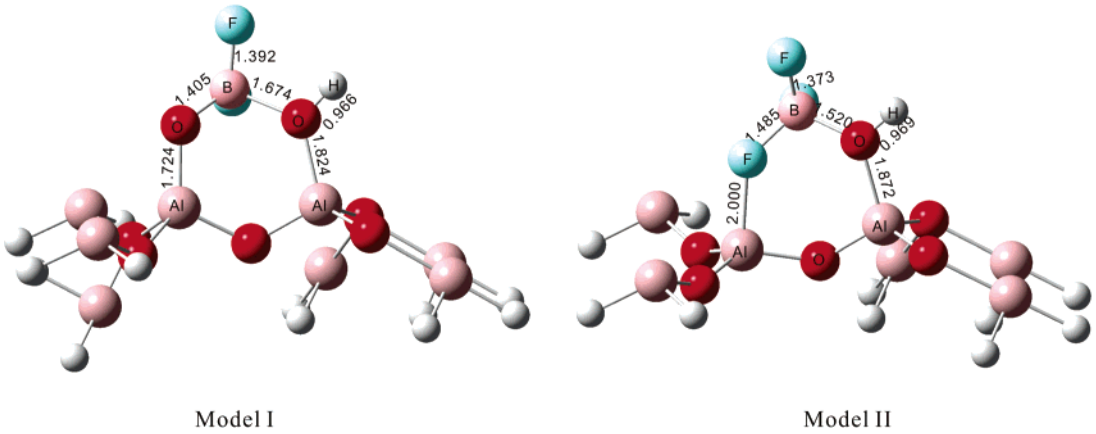

Model I Model II

Figure 8. B3LYP/DZVP2-optimized geometries of model I and model II (Brönsted acid sites formed on BF_3/γ-Al_2O_3). Selected bond lengths in angstroms are indicated.

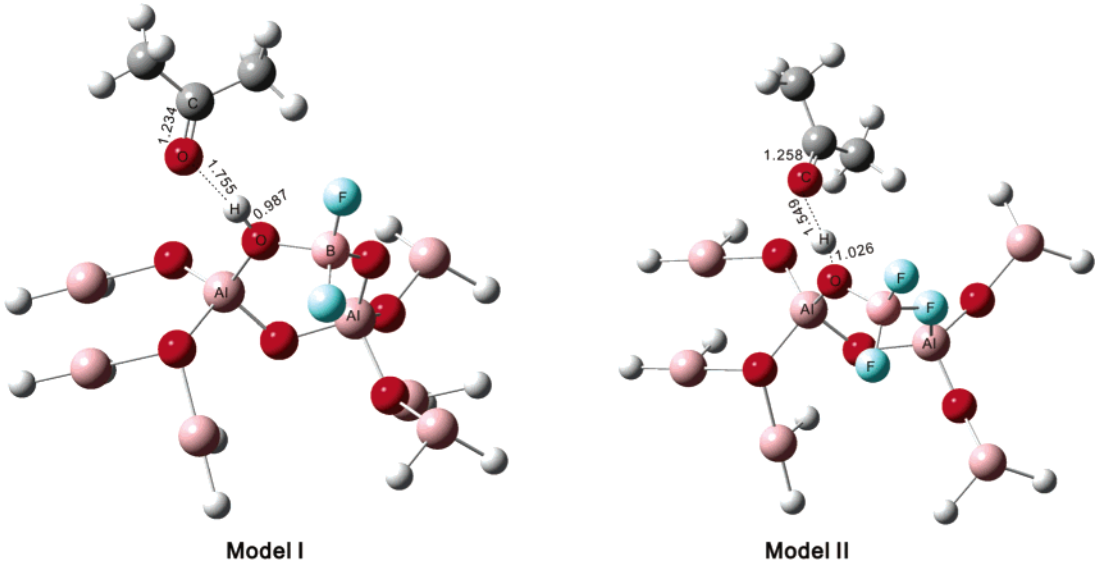

Model I **Model II**

Figure 9. B3LYP/DZVP2-optimized geometries of acetone adsorbed on model I and model II. Selected bond lengths in angstroms are indicated.

kcal/mol for model I after zero point thermal energy correction. We also calculated the PA value of zeolite HZSM-5, which is 294 kcal/mol. Haw et al. have predicted a similar PA value (294 kcal/mol) for the zeolite at the same level of calculations.[16] Obviously, the acid strength of model I is lower than that of HZSM-5.

In the optimized structure of Brönsted acid model II (see Figure 8), the B−F bond in the six-membered ring is enlarged to 1.485 Å compared with the other two B−F bonds (1.373 Å) because of the strong interaction between the F and Al atoms. The distance between the acidic proton and O atom is 0.969 Å, and the bond angle of Al−OH−B is 122.535°. The calculated PA value is 285 kcal/mol for model II, indicative of an acid strength stronger than that of zeolite HZSM-5.

We optimized the geometries of acetone adsorbed on the acidic proton of two Brönsted acid models, which are shown in Figure 9. There is strong hydrogen bonding between the Brönsted acidic proton of the BF_3/γ-Al_2O_3 catalyst and the carbonyl oxygen of adsorbed acetone. In the complex structure of model I, the O−H bond distance increases from 0.966 to 0.987 Å, the distance between the acidic proton and the carbonyl oxygen is 1.755 Å, and the C═O bond length increases from 1.224 to 1.234 Å after the adsorption of acetone. For acetone adsorbed on model II, an obvious change occurs in the complex structure. For example, the O−H bond length increases further to 1.026 Å, the distance between the carbonyl oxygen and the acidic proton decreases to 1.549 Å, and the C═O bond length increases further to 1.258 Å. Using theoretical calculation at the same computational level (B3lYP/DZVP2), Nicholas[16a] revealed a similar trend for acetone adsorbed on zeolite HZSM-5 and found that the C═O bond length was elongated to 1.239 Å. From the elongation extent of the C═O bond length of adsorbed acetone, the acid strength order of the two models compared with zeolite HZSM-5 can be predicted as follows: model I (1.234 Å) < HZSM-5 (1.239 Å) < model II (1.258 Å).

TABLE 1: Calculated Proton Affinity (PA) and ^{13}C Chemical Shift Data of 2-^{13}C-Acetone Adsorbed on Brönsted Acid Model I, Model II, and Zeolite HZSM-5 (the Corresponding Experimental ^{13}C Chemical Shifts Are Also Included)

	BF_3/γ-Al_2O_3 catalyst		
	model I	model II	HZSM-5
PA (kcal/mol)	318	285	294
computational ^{13}C chemical shift (ppm)	220.0	230.9	224.4
experimental ^{13}C chemical shift (ppm)	230		223.7[a]

[a] Taken from ref 13.

We also calculated the ^{13}C isotropic chemical shift of the carbonyl carbon for acetone adsorbed on the two proposed models and zeolite HZSM-5, and the corresponding results are listed in Table 1. The ^{13}C isotropic chemical shifts of carbonyl

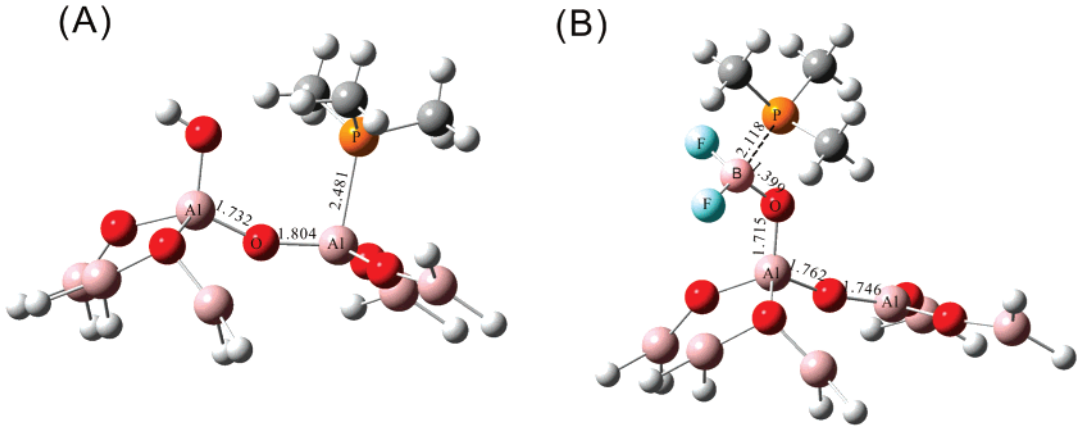

Figure 10. B3LYP/6-31G(d)-optimized geometries of TMP adsorbed on Lewis acid sites of parent γ-Al_2O_3 (A) and BF_3/γ-Al_2O_3 (B) catalysts. Selected bond lengths in angstroms are indicated.

carbon are 220.0 and 230.9 ppm for acetone adsorbed on models I and II, respectively. The corresponding chemical shift is 224.4 ppm for acetone adsorbed on zeolite HZSM-5, very close to the experimental value (223.7 ppm).[13]

Therefore, the calculated ^{13}C chemical shift data also suggest a similar acid strength order: model I < HZSM-5 < model II. Since the experimentally measured ^{13}C chemical shift (230 ppm) for 2-^{13}C-acetone adsorbed on our BF_3/γ-Al_2O_3 catalyst is very close to that calculated for model II, we believe that model II is the most plausible structure for Brönsted acid sites formed after the adsorption of BF_3 onto γ-Al_2O_3.

The complex structures of probe molecule adsorbed on Lewis acid sites were considered as well. The optimized geometries of TMP absorbed on Lewis acid sites of γ-Al_2O_3 and BF_3/γ-Al_2O_3 were shown in Figure 10. For TMP adsorbed on γ-Al_2O_3, the bond length between three-coordinate Al and P atoms is 2.481 Å, whereas the bond length between B and P atoms is shortened to 2.118 Å for TMP absorbed on BF_3/γ-Al_2O_3, indicative of a much stronger Lewis acidity of the BF_3/γ-Al_2O_3 catalyst compared with parent γ-Al_2O_3. The predicted ^{31}P NMR isotropic chemical shifts of TMP adsorbed on the Lewis acid sites of parent γ-Al_2O_3 and BF_3/γ-Al_2O_3 are −48 and −34 ppm, respectively, which are close to the corresponding experimental values (−51 and −26 ppm). Therefore, the agreement between experimental and theoretical calculations results strongly supports the proposed model III for Lewis acid sites formed on the BF_3/γ-Al_2O_3 catalyst.

Surface Modification of γ-Al_2O_3 by BF_3. Although there are three types of AlOH groups on the surface of γ-Al_2O_3 that might act as Brönsted acid sites, their acid strengths are not strong enough to protonate TMP and thus no resonance at −2 to −4 ppm arising from $TMPH^+$ ion was observed in the corresponding ^{31}P MAS NMR spectrum. Only Lewis acid sites, probably due to an unsaturated defect Al site (such as three-coordinate Al) present on the surface of γ-Al_2O_3, can be detected by the TMP probe molecule (at −51 ppm).[30]

After the adsorption of BF_3 onto the surface of γ-Al_2O_3, new Brönsted and Lewis acid sites appear, which are characterized by the two signals at −4 and −26 ppm in the ^{31}P NMR spectrum of TMP adsorbed on the catalyst, respectively. Obviously, the formation of new acid sites results from interaction between BF_3 and the surface of γ-Al_2O_3. On the basis of our NMR experimental results, the bridging Al−OH−B hydroxyl group is generated after the adsorption of BF_3 onto γ-Al_2O_3, we propose two possible pathways for the formation of Brönsted acid sites, which are shown in Scheme 1. The Brönsted acid site with a structure of model I is generated by the reaction of BF_3 with two neighboring surface AlOH groups and subsequent removal of one HF molecule, while the Brönsted acid site with a structure of model II is formed by the interaction of BF_3 with one AlOH group and one neighboring unsaturated Al defect site (such as three-coordinate Al). The presence of the Al−F bond in model II has been confirmed by our NMR experiments with the appearance of an ^{27}Al signal at −16 ppm and a ^{19}F signal at −180 ppm. Grey et al.[27] also found the formation of the Al−F−Al structure after the adsorption of chlorodifluoromethane gas onto the surface of γ-Al_2O_3. ^{13}C NMR of acetone adsorbed on BF_3/γ-Al_2O_3 catalyst suggests that the acid strength of the newly formed Brönsted acid site is stronger than zeolite HZSM-5 but still weaker than 100% H_2SO_4. Our theoretical calculations of both proton affinity and ^{13}C chemical shift of adsorbed acetone strongly confirm that model II is the most preferred structure of the Brönsted acid site present on the BF_3/γ-Al_2O_3 catalyst. It is noteworthy that the calculated ^{13}C chemical shift (230.9 ppm) of acetone adsorbed on model II agrees very well with the corresponding experimentally measured value (230 ppm). Therefore, we believe that Brönsted acid sites of the BF_3/γ-Al_2O_3 catalyst are most likely formed by the interaction of BF_3 with one AlOH group and one neighboring Al defect site.

Obviously, the coordination of a F atom with the Al defect site (in model II) might lead to the disappearance of the Al-containing Lewis acid sites that are originally present on the surface of γ-Al_2O_3. This corresponds to the disappearance of the −51 ppm signal and the appearance of a new signal at −26 ppm in the corresponding ^{31}P NMR spectra of TMP adsorbed on the γ-Al_2O_3 and BF_3/γ-Al_2O_3 catalysts, respectively. Our $^{31}P/^{27}Al$ TRAPDOR experiment indicates that the new signal should originate from a Lewis acid site that is not associated with Al. We suspect that the new Lewis acid site is generated by reaction of BF_3 with one AlOH group and subsequent elimination of one HF molecule (Scheme 2). In this case, a three-coordinate boron species ($-OBF_2$) is formed, which has been confirmed by ^{11}B MQ-MAS and $^{11}B/^{27}Al$ REDOR NMR experiments. Theoretical calculations of the adsorption complex of TMP strongly support the proposed model III for the Lewis acid site formed on BF_3/γ-Al_2O_3. Both the shorter B−P distance (compared with the Al−P distance) and the larger ^{31}P chemical shift for TMP adsorbed on BF_3/γ-Al_2O_3 indicate that the catalyst has a much stronger Lewis acid strength compared with parent γ-Al_2O_3.

Conclusion

The detailed structure and properties of acid sites formed on the surface of the BF_3/γ-Al_2O_3 catalyst are revealed by multinuclear solid-state NMR techniques as well as DFT quantum chemical calculations. ^{11}B MQ-MAS and $^{11}B/^{27}Al$ REDOR NMR experiments indicate the presence of three-coordinate and four-coordinate boron species on the BF_3/γ-Al_2O_3 catalysts that are all in close proximity to Al atoms, implying that B−O−Al linkages are formed. A new signal at 3.7 ppm, showing both $^1H/^{11}B$ and $^1H/^{27}Al$ TRAPDOR effects, appears in the ^1H spectrum of the catalyst. This signal is due to the bridging B−OH−Al group that most likely acts as the Brönsted acid site. As revealed by ^{31}P MAS and $^{31}P/^{27}Al$ TRAPDOR NMR of TMP, both Brönsted and Lewis acid sites are present on the surface of BF_3/γ-Al_2O_3 with the latter arising from three-coordinate $-OBF_2$ species. ^{13}C NMR of 2-^{13}C-acetone adsorbed on BF_3/γ-Al_2O_3 shows that the Brönsted acid strength of the catalyst is slightly higher than that of the bridging OH group in zeolite HZSM-5 but still weaker than that of 100% H_2SO_4. In combination with DFT calculations, the detailed structures of Brönsted and Lewis acid sites formed on the surface of the BF_3/γ-Al_2O_3 catalyst are revealed and the predicted acid strengths of these sites are in good agreement with experimental observations.

Acknowledgment. We are very grateful for the support of the National Natural Science Foundation of China (20425311, 20273082, and 20425312) and State Key Fundamental Research Program (2002CB713806) of China.

References and Notes

(1) Corma, A.; Martinez, A. *Catal. Rev.—Sci. Eng.* **1993**, *35*, 483.
(2) Weitkamp, J.; Traa, Y. *Catal. Today* **1999**, *49*, 193.
(3) Hommeltoft, S. I. *Appl. Catal., A* **2001**, *221*, 421.
(4) (a) Corma, A.; Martinez, A.; Martinez, C. *J. Catal.* **1994**, *146*, 185. (b) Cardona, F.; Gnep, N. S.; Guisnet, M.; Szabo, G.; Nascimento, P. *Appl. Catal., A* **1995**, *128*, 243.
(5) (a) Okuhara, T.; Yamashita, M.; Na, K.; Misono, M. *Chem. Lett.* **1994**, 1451. (b) Essayem, N.; Kieger, S.; Coudurier, G.; Vedrine, J. *Stud. Surf. Sci. Catal.* **1996**, *101*, 591.
(6) (a) Guo, C.; Yao, S.; Cao, J.; Qian, Z. *Appl. Catal., A* **1994**, *107*, 229. (b) Corma, A.; Juan-Rajadell, M. I.; López-Nieto, J.; Martinez, A.; Martinez, C. *Appl. Catal., A* **1994**, *111*, 175.
(7) Tanabe, K.; Hölderich, W. F. *Appl. Catal., A* **1999**, *181*, 399.
(8) Michael, D.; King, D.; Sanderson, W. U.S. Patent 5,157,197, 1992.
(9) Drago, R. S.; Petrosius, S. C.; Chronister, C. W. *Inorg. Chem.* **1994**, *33*, 367.
(10) Marczewski, M.; Marzewska, H.; Witoslawski, K. *Bull. Soc. Chim. Fr.* **1991**, 366.
(11) Haw, J. F.; Nicholas, J. B.; Xu, T.; Beck, L. W.; Ferguson, D. B. *Acc. Chem. Res.* **1996**, *29*, 259.
(12) (a) Hunger, M. *Catal. Rev.—Sci. Eng.* **1997**, *39*, 345. (b) Hunger, M.; Weitkamp, J. *Angew. Chem., Int. Ed.* **2001**, *40*, 2954. (c) Xu, M.; Arnold, A.; Buchholz, A.; Wang, W.; Hunger, M. *J. Phys. Chem. B* **2002**, *106*, 12140.
(13) (a) Xu, T.; Kob, N.; Drago, R. S.; Nicholas, J. B.; Haw, J. F. *J. Am. Chem. Soc.* **1997**, *119*, 12231. (b) Krawietz, T.; Lin, P.; Lotterhos, K. E.; Torres, P. D.; Barich, D. H.; Clearfield, A.; Haw, J. F. *J. Am. Chem. Soc.* **1998**, *120*, 8502.
(14) Haw, J. F.; Xu, T.; Nicholas, J. B.; Gorgune, P. W. *Nature* **1997**, *389*, 832.
(15) (a) Zhang, J.; Nicholas, J. B.; Haw, J. F. *Angew. Chem., Int. Ed.* **2000**, *39*, 18. (b) Venkatraman, T. N.; Luigi, D.-P.; Song, W.; Barich, D. H.; Nicholas, J. B. *J. Am. Chem. Soc.* **2000**, *122*, 12561.
(16) (a) Nicholas, J. B. *Top. Catal.* **1999**, *9*, 181. (b) Ehresmann, J. O.; Wang, W.; Herreros, B.; Luigi, D. P.; Venkatraman, T. N.; Song, W.; Nicholas, J. B.; Haw, J. F. *J. Am. Chem. Soc.* **2002**, *124*, 10868.
(17) Imai, T. U.S. Patent 4,407,731, 1983.
(18) Grey, C. P.; Vega, A. J. *J. Am. Chem. Soc.* **1995**, *117*, 8232.
(19) Amoureux, J. P.; Fernandez, C.; Steuernagel, S. *J. Magn. Reson., Ser. A* **1996**, *123*, 116.
(20) Massiot, D.; Fayon, F.; Capron, M.; King, I.; Le Calve, S.; Alonso, B.; Durand, J. O.; Bujoli, B.; Gan, Z.; Hoatson, G. *Magn. Reson. Chem.* **2002**, *40*, 70.
(21) (a) Gullion, T.; Schaefer, J. *J. Magn. Reson.* **1989**, *81*, 196. (b) Gullion, T.; Schaeffer, J. *J. Magn. Reson.* **1991**, *92*, 439.
(22) Zhou, R. S.; Snyder, R. L. *Acta Crystallogr., Sect. B* **1991**, *47*, 617.
(23) Gorenstein, D. G. *Phosphorus-31 NMR: principles and applications*; Academic Press: Orlando, FL, 1984.
(24) Frisch, M. J.; Trucks, G. W.; Schlegel, H. B.; Chen, W.; Wong, M. W.; Gonzalez, C.; Pople, J. A. *Gaussian03*; Gaussian, Inc.: Pittsburgh, PA, 2003.
(25) (a) Knözinger, H.; Ratnasamy, P. *Catal. Rev.—Sci. Eng.* **1978**, *17*, 31. (b) Deng, F.; Wang, G.; Du, Y.; Ye, C.; Kong, Y.; Li, X. *Solid State Nucl. Magn. Reson.* **1997**, *7*, 281.
(26) Decanio, E. C.; Edwards, J. C.; Bruno, J. W. *J. Catal.* **1994**, *148*, 76.
(27) Chupas, P. J.; Grey, C. P. *J. Catal.* **2004**, *224*, 69.
(28) Medek, A.; Harwood, J. S.; Frydman, L. *J. Am. Chem. Soc.* **1995**, *117*, 12779.
(29) Lunsford, J. H.; Rothwell, W. P.; Shen, W. *J. Am. Chem. Soc.* **1985**, *107*, 1540.
(30) Yang, J.; Zhang, M.; Deng, F.; Luo, Q.; Ye, C. *Chem. Commun.* **2003**, 884.
(31) Kao, H. K.; Grey, C. P. *Chem. Phys. Lett.* **1996**, *259*, 459.
(32) (a) Biaglow, A.; Gorte, R.; Kokotailo, G.; White, D. *J. Catal.* **1994**, *148*, 779. (b) Biaglow, A.; Gorte, R.; White, D. *J. Catal.* **1994**, *150*, 221.